Petrophysical Evaluation of Lacustrine Shales in the Cooper Basin, Australia*

Melissa Vallee[1]

Search and Discovery Article #41205 (2013)
Posted October 18, 2013

*Adapted from extended abstract prepared in conjunction with poster presentation at AAPG Annual Convention and Exhibition, Pittsburgh, Pennsylvania, May 19-22, 2013

[1]Unconventional Resources-Subsurface Services, Santos Ltd, Adelaide, SA, Australia (melissa.vallee@santos.com)

Abstract

While the petrophysical evaluation of conventional reservoirs has become routine, the assessment of unconventional reservoirs including gas shales, tight sandstones, and deep dry coals in the Cooper Basin has required the use of the latest logging technology and core-analysis techniques. Estimation of the gas content contained within the connected porosity of these reservoirs and formulation of an effective production strategy requires the integration of data from multiple disciplines, including organic geochemistry, tight-rock analysis, organic petrology, and geomechanics.

Introduction

Although the Cooper Basin has been explored and exploited for more than 40 years, the current logging suite for conventional sandstones still only comprises a handful of logs (gamma ray, resistivity, neutron-density, sonic), sometimes formation tests and rotary sidewall cores, and usually involves one or two service companies. By way of comparison, during the drilling of six wells used to assess the unconventional gas potential of the Nappamerri Trough in the Cooper Basin in East-Central Australia, a diverse suite of specialised petrophyisical imaging and mineralogy logs were acquired; three hundred feet of core were cut, and eight service companies (Weatherford, Terratek, DigitalCore, CBM Solutions, GeoGAS, GeoTek, CSIRO, Amintek) were engaged to undertake core analyses, including retort analyses for fluid saturation, geomechanical tests, crushed bulk density, as received gas-filled porosity, pressure-decay permeability, bulk X-Ray Diffraction (XRD), organic petrology, RockEval, low and high resolution computer tomography CT scans.

The purpose of this article is to illustrate how the Santos petrophysics team has adopted and adapted the different techniques and technologies in the market to evaluate a challenging and still not well understood lacustrine shale play, such as found in the Cooper Basin.

Objectives

- Determine the organic content, mineral content, porosity, permeability, amount of adsorbed gas, and geomechanical properties of the Murteree Shale.
- Establish the shale gas potential of the basin using the latest logging technologies and core-analysis techniques.
- Calculate rock brittleness in order to identify intervals that will prove easier to stimulate using hydraulic fracturing treatments and intervals that will prove potential barriers.
- Generate petrophysical workflows for the evaluation of lacustrine shales in the Cooper Basin.

Background

The intracratonic Cooper Basin represents a Late Carboniferous to Triassic depositional episode terminated at the end of the Middle Triassic with widespread compressional folding, regional uplift, and erosion; this area then experienced development of the Jurassic-Cretaceous Eromanga Basin (Alexander, et.al., 2006). It is approximately 560 km long and 300 km wide. Three major depocentres (Patchawarra, Nappamerri, and Tenappera troughs) are filled with Permo-Carboniferous and Triassic sediments and separated by structural ridges.

The Lower Permian succession is in part characterised by lacustrine mudrocks (laminated siltstones and mudstones) associated with a basin-centered gas accumulation in the Nappamerri Trough. The high geothermal gradient in the Nappamerri Trough makes the organic matter in the mudrocks quite mature and also contributes to the simplicity in the mineralogy of the clays (Lemon, 2006). Strong diagenetic imprint also has consequences on the geomechanical properties of the formations, resulting in higher rock strength.

Procedures

In order to understand the potential of the shale reservoirs in the Cooper Basin a list of specialised logs and core analyses were acquired to determine the organic content, mineral content, porosity, permeability, fluid saturations, amount of adsorbed gas, and the geomechanical properties of these shales.

Organic and Mineral Content Estimation

Total organic content (TOC) was calculated in core shale samples using LECO Organic Carbon and Rock-Eval II Pyrolysis techniques. Furthermore, these samples also underwent individual methane adsorption and sorption isotherm analyses at reservoir temperature. TOC was best determined by direct combustion of samples in a carbon analyzer at about 1000^{o}C. Rock- Eval II pyrolysis was used to determine kerogen type, kerogen maturity, and the amount of free hydrocarbons. Prepared samples were heated to 300^{o}C to determine the amount of free hydrocarbons (S1) that is thermally distilled. The amount of pyrolyzable hydrocarbons (S2) was measured in an inert environment from 300^{o}C to 550^{o}C. Tmax (maturity indicator) is the temperature of maximum S2 generation. Carbon dioxide generated during the S2 pyrolysis (indicator

of kerogen oxidation) was collected up to a temperature of 390^{o}C (S3). Hydrogen Index (HI=S2x100/TOC) and Oxygen Index (OI=S3x100/TOC) were used as kerogen type indicators when plotted on a Van Krevelen type diagram.

Quantitative bulk and fine fraction XRD analyses were performed on shale core samples in order to determine the mineralogical composition of the shales. TOC and mineral content were also calculated using pulsed neutron elemental spectroscopy logging tools. This tool was able to provide a formation weight percentage of elemental carbon. These measurements when combined with the elements that were quantifiable through the measure of the gamma energy spectrum allowed the estimation of the lithology and mineralogy of the formation. The excess carbon from the mineralogy log that was not associated with carbonaceous minerals was back calculated as proportional to TOC.

Porosity and Fluid Saturations Calculations

Free-gas storage capacity (gas-filled porosity (gfp)) was estimated in both the organic and inorganic pore framework in core shale samples using Tight Rock Analyses techniques. One of them was the modified retort analysis for fluid saturation. The traditional retort fluid extraction method has been used for the evaluation of fluid saturations on conventional reservoirs but has been modified for use in tight shale applications. The technique uses heat to vaporise the pore fluids and extract them from the sample and measures the volume of extracted water and oil directly by condensing the vapours in a receiver container. The modification for tight shale applications is mainly the crushing and weighing of the samples before being placed in the retort oven. During the retort process, water and oil, free and surface-bound, are vaporized, condensed, separated, and measured using three different temperatures. Volume of gas was measured on a separated split of the same crushed material, using Boyle's law helium porosimetry. With the experiment, it was possible to obtain values for total porosity, effective gas-filled porosity, clay-bound water, and capillary-bound water.

X-ray computer tomography techniques were also used to visualise the pore network in the shales in 3 dimensions. DigitalCore has developed or improved this technique to be able to determine connected macroporosity in the shales in the Cooper Basin. Full diameter shale cores were subsampled with mini-plugs, taking in account that the smaller the plug size dimension, the higher the resolving power of the technique. DigitalCore uses a high resolution X-ray micro-ct device to capture X-ray slices or tomograms of the shale samples. The technique is based on the X-ray attenuation provided by cesium iodide occupying vacant pore space in the shale. Mini-plugs of three millimetres were cut and scanned in their native stage, and then they were impregnated with X-ray attenuation fluid and scanned again. The difference in attenuation between the native and saturated images defines the porosity at each slice. Also scanning electron microscopy images (SEM) with back-scattered electron detector (BSE) were taken by DigitalCore using the same three millimetres miniplug shale samples to identify the type of clays and confirm the presence of intercrystalline porosity.

Nuclear Magnetic Resonance was acquired as a matrix independent porosity measurement, able to quantify the fluids distribution in macro- and mesopores of the formations.

Permeability Estimations

Data for permeability experiments was acquired and analysed using CBM Solutions' proprietary software. Shale samples of three-centimetre diameter were cut from full core. Initially permeability to argon was measured using a variation of the pulse-decay technique with varying confining pressures to quantify the permeability of the formation under reservoir conditions, but the limitations of the test prevented the collection of enough data; so therefore pulse decay permeability to helium was instead measured. The equipment used was able to measure permeabilities as low as 0.1 nd. Also, pressure decay permeability experiments on unconfined crushed samples at ambient pressure and temperature were carried out.

Geomechanical Properties

The geomechanical properties of the shales have been shown to be sensitive to factors such as composition, organic content, pore pressure, and stress history. Core shale samples underwent triaxial compression tests to calculate Young's Modulus, Poisson's Ratio, and Unconfined Compressive Strength. The first two measure stiffness and deformation, respectively, and, when combined, can reflect the ability of the rocks to fail under stress and maintain a fracture once the rock strength fails. This can be defined as brittleness. Brittle shales are more likely to be naturally fractured and will also be more likely to respond well to hydraulic fracturing treatments. Unconfined Compressive Strength combined with Young's Modulus was used as an indicator to identify the shale intervals that will propagate the fractures or attenuate their propagation. These properties were also determined from acoustic log measurements. Based on these properties, the value of horizontal stress was calculated using a poroelastic equation for use in fracture stimulation.

Results

Geochemical analyses showed peak gas generation from dispersed type III kerogen in the shales in the Cooper Basin; with thermal maturities greater than 1.4%, localizing this part of the basin within the dry gas zone. Plots of total gas yield versus vitrinite reflectance (Figure 1) indicate that about 80% of the maximum quantity of gas available from the type III kerogen is expelled upon reaching a maturity of 2%.

Fluid saturations within the total and effective pore volume were defined through tight rock retort analyses. Mobile water and hydrocarbons, clay-bound water, structural water, gas-filled porosity, and free-gas calculations are shown in Table 1.

Mineralogy was identified by examination of XRD analyses, CT-scans, and BSE microscopy images. The XRD patterns in Figure 2 indicate the presence of illite, kaolinite, quartz, siderite and traces of heavy minerals as rutile and/or anatase. These minerals remain homogeneously distributed, except for siderite, which presence changes with changes in depth.

BSE microscopy images were used to visualise the fabric of the samples. Figure 3 shows a collage of BSE shale images at different scales. These images indicate that most of the porosity is developed within an illite-kaolinite intercrystalline matrix and only a small fraction of porosity is preserved in the macropores of vitrinite particles. Digital micro-ct analysis confirmed that there is a small amount of connected

porosity and therefore potential free-gas storage associated with inorganic phyllosilicate framework pores in a mix of illite and kaolinite detrital clays.

NMR interpretation show values of total porosity in the shale intervals between 2 and 6% (depending on the mineralogical composition of the rock) and small amounts of effective porosity, ranging between 1 and 3.5%. However, most of this effective porosity was interpreted as being filled by irreducible fluids. It is alleged that in NMR gradient tools gas T2 response is affected by diffusion and this could explain why the tool is not detecting most of the free gas that was calculated by retort analysis experiments. Another reason for the underestimation of free gas in the shale intervals could be that the fixed T2 cut-off of 32 ms used for the interpretation is a bit pessimistic. Consequently, some of the gas could be distributed or interpreted as being in the bulk volume irreducible (BVI) of the spectrum and only a very small part of gas interpreted as being distributed in the movable part (BVM). Additional NMR modelling (i.e., 2D NMR or Density/NMR integration) needs to be completed to define a more appropriate T2 distribution time for these shales.

Permeability results from pressure-decay experiments on unconfined crushed samples at ambient pressure and temperature show values ranging between 100 and 140 nd, whilst results from in situ pulse-decay permeability experiments on confined plugs at reservoir pressure and temperature conditions were much lower, on the order of 1 nd. Evidently there is a variation of permeability with applied stress; therefore, at net overburden pressure, the matrix permeability of these rocks are very low.

The mechanical properties of the shales in the Cooper Basin proved to be strongly influenced by the mineralogy of the formation. Intervals with higher quartz content have demonstrated to be the easiest to fracture stimulate, with lower Poisson's Ratio and higher Young's Modulus values; whilst the carbonaceous-shalier intervals have proven to be more ductile, acting as barriers and attenuating the propagation of the fractures.

Conclusions

- The Cooper Basin Permian lacustrine mudrocks intersected in the studied wells are characterized by a simple mineralogy and homogeneous lithofacies. This demonstrates that diagenesis has had a strong impact on the mineralogy of the clays and the development of siderite.
- Free-gas storage capacity within the mudrocks is associated with inorganic porosity developed within intercrystalline pore spaces of diagenetically altered clays rather than organic-derived porosity.
- The shale gas potential of the Cooper Basin lacustrine mudrocks is related to the dynamics of the basin-centered gas system developed within the Nappamerri Trough, variation of kerogen type, thermal maturity trends and a spectrum of inorganic and organic-derived poro-perm networks that are both variable and complex.
- The application of the traditional Delta Log R Passey's technique to assess the potential of the lacustrine shales in the Cooper Basin became a challenge due to the high maturity of the basin. The learning curve is still growing, but a moderate understanding of these mudrocks was achieved only through the integration of geochemical analyses, XRD graphs, geomechanical experiments, NMR data, spectroscopy, and sonic logs, just to name a few.

Selected References

Alexander, E.M., Sansome, A., and Cotton, T.B., 2006, Lithostratigraphy and environments of deposition, *in* Alexander, E.M. and Cotton, T.B., Petroleum Geology of South Australia, v. 2: Eromanga Basin.

Handwerger, D.A., Suarez-Rivera, R., Vaughn, K.I., and Keller, J.F., 2011, Improved petrophysical core measurements on tight shale reservoirs Using retort and crushed samples: SPE Annual Technical Conference and Exhibition. Denver, Colorado, USA.

Lemon, N.M., 2006, Geology of the Cooper Basin area: A snapshot of 300 million years: Santos G&E Conference, Santos Ltd. internal presentation.

Passey, Q.R., Creaney, S., Kulla, J.B., Moretti, F.J., and Stroud, J.D., 1990, A practical model for organic richness from porosity and pesistivity logs: AAPG Bulletin, v. 74, p. 1777-1794.

Acknowledgements

Special thanks to the Unconventional Resources Team, Santos and its Joint Venture Parties for allowing publishing this work. I am indebted to Suryakant Bulgauda for his invaluable technical assistance in petrophysics and editorial feedback.

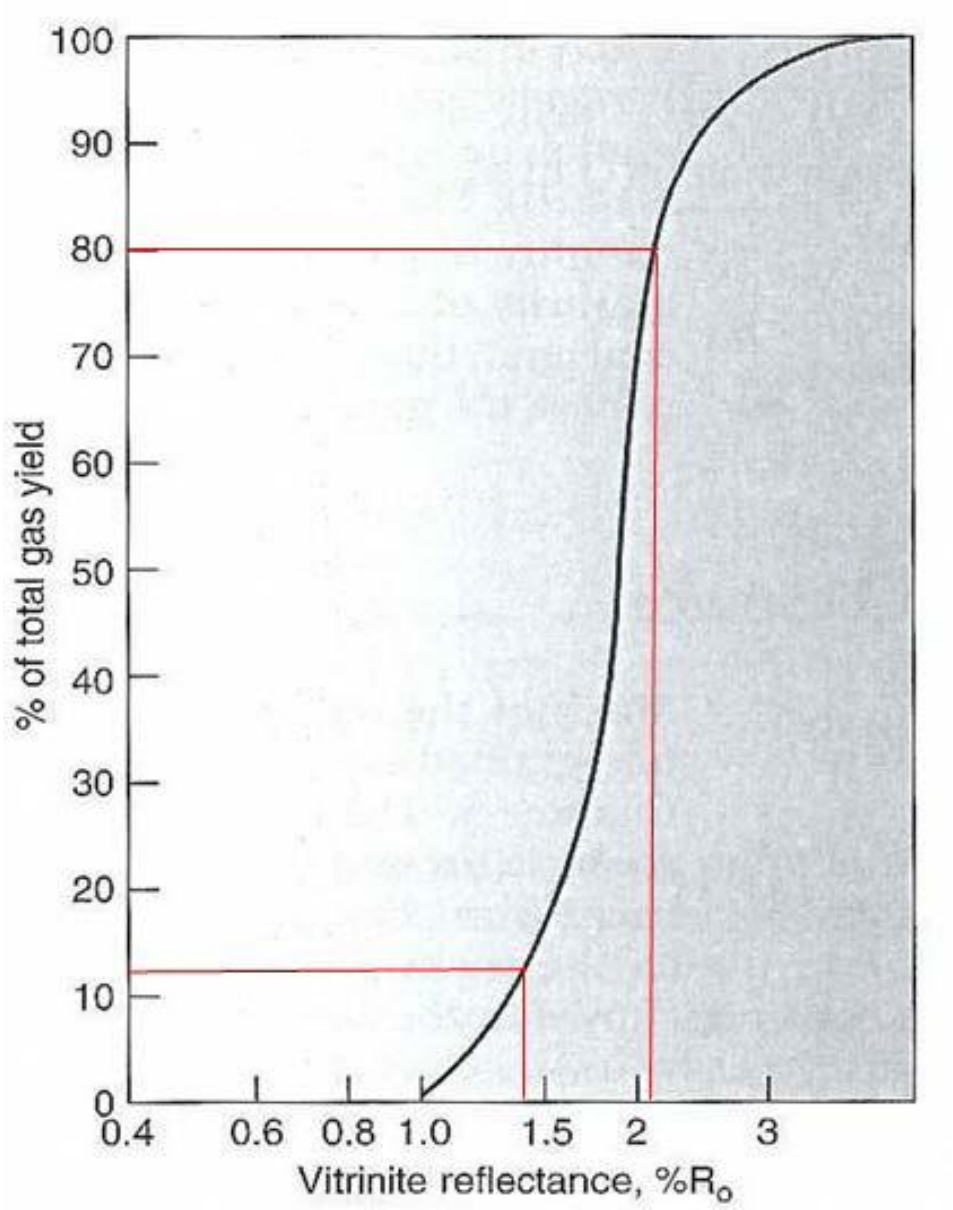

Figure 1. Plot of total gas yield versus vitrinite reflectance.

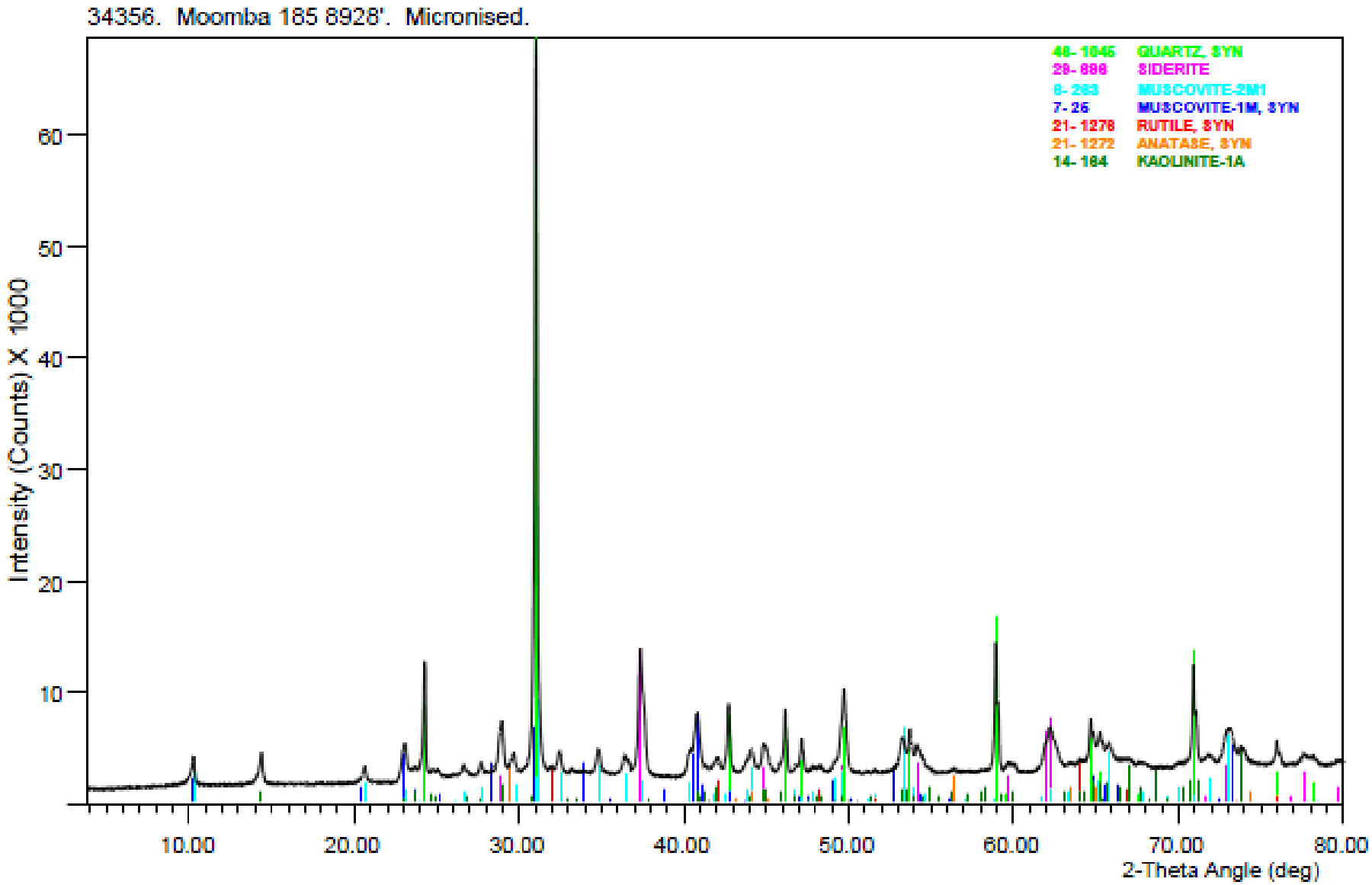

Figure 2. XRD patterns of shale samples in the Murteree Shale in the Cooper Basin.

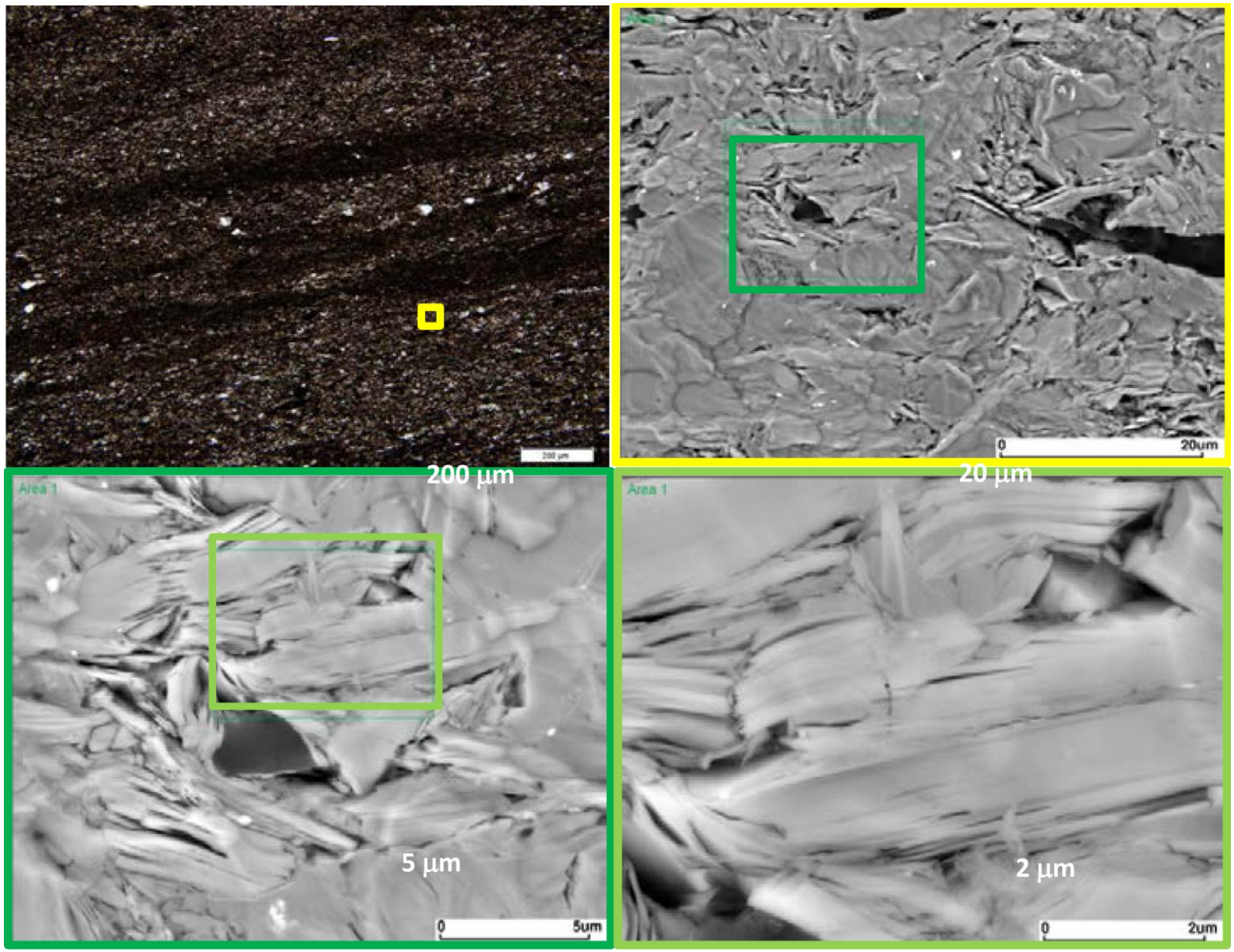

Figure 3. BSE microscopy of a shale sample in the Cooper Basin at different magnifications, showing potential free-gas storage associated with inorganic phyllosilicate framework pores in a mix of illite and kaolinite detrital clays.

Pore Volume		Porosity		Effective Saturations			Total Saturations			Clay Bound Water		Structural Water		"Reported" Bound Clay Water (% of BV)
Effective Pore Volume (cc)	Total Pore Volume (cc)	T1 Effective Porosity (% of V_B)	T2 Total Porosity (% of V_B)	Gas Saturation (%)	Water Saturation (%)	Mobile Hydrocarbon Saturation (%)	Gas Saturation (%)	Water Saturation (%)	Mobile Hydrocarbon Saturation (%)	Final Clay Water Volume (cc)	Clay Water (% of V_B)	Final Structural Water Volume (cc)	Structural Water (% of V_B)	Structural Water + Clay Water
0.201	0.280	1.80	2.51	51.00	39.09	9.91	36.60	56.29	7.11	0.100	0.89	0.842	7.52	8.41
0.329	0.410	2.90	3.60	72.71	24.26	3.03	58.44	39.12	2.44	0.100	0.88	0.843	7.42	8.29
0.308	0.385	2.73	3.41	70.87	22.65	6.47	56.71	38.11	5.18	0.100	0.88	0.832	7.35	8.23
0.326	0.383	2.95	3.47	77.15	16.71	6.14	65.65	29.12	5.22	0.078	0.71	0.711	6.45	7.15
0.256	0.318	2.27	2.82	57.94	34.25	7.80	46.71	47.00	6.29	0.089	0.79	0.910	8.07	8.86
0.169	0.212	1.56	1.95	51.57	36.65	11.78	41.22	49.36	9.42	0.055	0.51	0.698	6.44	6.95
0.279	0.350	2.51	3.14	61.87	30.98	7.15	49.41	44.88	5.71	0.100	0.90	0.943	8.47	9.36
0.377	0.437	3.39	3.92	76.16	18.55	5.30	65.81	29.61	4.58	0.078	0.70	0.766	6.88	7.58
0.271	0.357	2.34	3.09	65.15	27.47	7.38	49.44	44.96	5.60	0.111	0.96	0.988	8.55	9.52
0.294	0.361	2.61	3.21	66.05	27.16	6.79	53.79	40.68	5.53	0.100	0.89	0.843	7.49	8.38

Table 1: Distribution of pore volume and fluid saturations.